

Study of open-charm decay and radiative transitions of the X(3872)

- M. Ablikim¹, M. N. Achasov^{10,e}, P. Adlarson⁶³, S. Ahmed¹⁵, M. Albrecht⁴, A. Amoroso^{62A,62C}, Q. An^{59,47}, Anita²¹, Y. Bai⁴⁶, O. Bakina²⁸, R. Baldini Ferroli^{23A}, I. Balossino^{24A}, Y. Ban³⁷, K. Begzsuren²⁶, J. V. Bennett⁵, N. Berger²⁷, M. Bertani^{23A}, D. Bettoni^{24A}, F. Bianchi^{62A,62C}, J. Biernat⁶³, J. Bloms⁵⁶, A. Bortone^{62A,62C}, I. Boyko²⁸, R. A. Briere⁵, H. Cai⁶⁴, X. Cai^{1,47}, A. Calcaterra^{23A}, G. F. Cao^{1,51}, N. Cao^{1,51}, S. A. Cetin^{50B}, J. F. Chang^{1,47}, W. L. Chang^{1,51}, G. Chelkov^{28,c,d}, D. Y. Chen⁶, G. Chen¹, H. S. Chen^{1,51}, M. L. Chen^{1,47}, S. J. Chen³⁵, X. R. Chen²⁵, Y. B. Chen^{1,47}, W. Cheng^{62C}, G. Cibinetto^{24A}, F. Cossio^{62C}, X. F. Cui³⁶, H. L. Dai^{1,47}, J. P. Dai^{41,i}, X. C. Dai^{1,51}, A. Dbeysi¹⁵, R. B. de Boer⁴, D. Dedovich²⁸, Z. Y. Deng¹, A. Denig²⁷, I. Denysenko²⁸, M. Destefanis^{62A,62C}, F. De Mori^{62A,62C}, Y. Ding³³, C. Dong³⁶, J. Dong^{1,47}, L. Y. Dong^{1,51}, M. Y. Dong^{1,47,51}, S. X. Du⁶⁷, J. Fang^{1,47}, S. S. Fang^{1,51}, Y. Fang¹, R. Farinelli^{24A,24B}, L. Fava^{62B,62C}, F. Feldbauer⁴, G. Felici^{23A}, C. Q. Feng^{59,47}, M. Fritsch⁴, C. D. Fu¹, Y. Fu¹, X. L. Gao^{59,47}, Y. Gao³⁷, Y. Gao⁶⁰, Y. G. Gao⁶, I. Garzia^{24A,24B}, E. M. Gersabeck⁵⁴, A. Gilman⁵⁵, K. Goetzen¹¹, L. Gong³⁶, W. X. Gong^{1,47}, W. Gradl²⁷, M. Greco^{62A,62C}, L. M. Gu³⁵, M. H. Gu^{1,47}, S. Gu², Y. T. Gu¹³, C. Y. Guan^{1,51}, A. Q. Guo²², L. B. Guo³⁴, R. P. Guo³⁹, Y. P. Guo²⁷, A. Guskov²⁸, S. Han⁶⁴, T. T. Han⁴⁰, T. Z. Han^{9,j}, X. Q. Hao¹⁶, F. A. Harris⁵², K. L. He^{1,51}, F. H. Heinsius⁴, T. Held⁴, Y. K. Heng^{1,47,51}, M. Himmelreich^{11,h}, T. Holtmann⁴, Y. R. Hou⁵¹, Z. L. Hou¹, H. M. Hu^{1,51}, J. F. Hu^{41,i}, T. Hu^{1,47,51}, Y. Hu¹, G. S. Huang^{59,47}, L. Q. Huang⁶⁰, X. T. Huang⁴⁰, N. Huesken⁵⁶, T. Hussain⁶¹, W. Ikegami Andersson⁶³, W. Imoehl²², M. Irshad^{59,47}, S. Jaeger⁴, S. Janchiv^{26,l}, Q. Ji¹, Q. P. Ji¹⁶, X. B. Ji^{1,51}, X. L. Ji^{1,47}, H. B. Jiang⁴⁰, X. S. Jiang^{1,47,51}, X. Y. Jiang³⁶, J. B. Jiao⁴⁰, Z. Jiao¹⁸, S. Jin³⁵, Y. Jin⁵³, T. Johansson⁶³, N. Kalantar-Nayestanaki³⁰, X. S. Kang³³, R. Kappert³⁰, M. Kavatsyuk³⁰, B. C. Ke^{42,1}, I. K. Keshk⁴, A. Khoukaz⁵⁶, P. Kiese²⁷, R. Kiuchi¹, R. Kliemt¹¹, L. Koch²⁹, O. B. Kolcu^{50B,g}, B. Kopf⁴, M. Kuemmel⁴, M. Kuessner⁴, A. Kupsc⁶³, M. G. Kurth^{1,51}, W. Kühn²⁹, J. J. Lane⁵⁴, J. S. Lange²⁹, P. Larin¹⁵, L. Lavezzi^{62C}, H. Leithoff²⁷, M. Lellmann²⁷, T. Lenz²⁷, C. Li³⁸, C. H. Li³², Cheng Li^{59,47}, D. M. Li⁶⁷, F. Li^{1,47}, G. Li¹, H. B. Li^{1,51}, H. J. Li^{9,j}, J. L. Li⁴⁰, J. Q. Li⁴, Ke Li¹, L. K. Li¹, Lei Li³, P. L. Li^{59,47}, P. R. Li³¹, W. D. Li^{1,51}, W. G. Li¹, X. H. Li^{59,47}, X. L. Li⁴⁰, Z. B. Li⁴⁸, Z. Y. Li⁴⁸, H. Liang^{59,47}, H. Liang^{1,51}, Y. F. Liang⁴⁴, Y. T. Liang²⁵, L. Z. Liao^{1,51}, J. Libby²¹, C. X. Lin⁴⁸, B. Liu^{41,i}, B. J. Liu¹, C. X. Liu¹, D. Liu^{59,47}, D. Y. Liu^{41,i}, F. H. Liu⁴³, Fang Liu¹, Feng Liu⁶, H. B. Liu¹³, H. M. Liu^{1,51}, Huanhuan Liu¹, Huihui Liu¹⁷, J. B. Liu^{59,47}, J. Y. Liu^{1,51}, K. Liu¹, K. Y. Liu³³, Ke Liu⁶, L. Liu^{59,47}, L. Y. Liu¹³, Q. Liu⁵¹, S. B. Liu^{59,47}, T. Liu^{1,51}, X. Liu³¹, Y. B. Liu³⁶, Z. A. Liu^{1,47,51}, Z. Q. Liu⁴⁰, Y. F. Long³⁷, X. C. Lou^{1,47,51}, H. J. Lu¹⁸, J. D. Lu^{1,51}, J. G. Lu^{1,47}, X. L. Lu¹, Y. Lu¹, Y. P. Lu^{1,47}, C. L. Luo³⁴, M. X. Luo⁶⁶, P. W. Luo⁴⁸, T. Luo^{9,j}, X. L. Luo^{1,47}, S. Lusso^{62C}, X. R. Lyu⁵¹, F. C. Ma³³, H. L. Ma¹, L. L. Ma⁴⁰, M. M. Ma^{1,51}, Q. M. Ma¹, R. Q. Ma^{1,51}, R. T. Ma⁵¹, X. N. Ma³⁶, X. X. Ma^{1,51}, X. Y. Ma^{1,47}, Y. M. Ma⁴⁰, F. E. Maas¹⁵, M. Maggiora^{62A,62C}, S. Maldaner²⁷, S. Malde⁵⁷, Q. A. Malik⁶¹, A. Mangoni^{23B}, Y. J. Mao³⁷, Z. P. Mao¹, S. Marcello^{62A,62C}, Z. X. Meng⁵³, J. G. Messchendorp³⁰, G. Mezzadri^{24A}, T. J. Min³⁵, R. E. Mitchell²², X. H. Mo^{1,47,51}, Y. J. Mo⁶, N. Yu. Muchnoi^{10,e}, H. Muramatsu⁵⁵, S. Nakhoul^{11,h}, Y. Nefedov²⁸, F. Nerling^{11,h}, I. B. Nikolaev^{10,e}, Z. Ning^{1,47}, S. Nisar^{8,k}, S. L. Olsen⁵¹, Q. Ouyang^{1,47,51}, S. Pacetti^{23B}, Y. Pan⁵⁴, Y. Pan^{59,47}, M. Papenbrock⁶³, A. Pathak¹, P. Patteri^{23A}, M. Pelizaeus⁴, H. P. Peng^{59,47}, K. Peters^{11,h}, J. Pettersson⁶³, J. L. Ping³⁴, R. G. Ping^{1,51}, A. Pitka⁴, R. Poling⁵⁵, V. Prasad^{59,47}, H. Qi^{59,47}, M. Qi³⁵, T. Y. Qi², S. Qian^{1,47}, W.-B. Qian⁵¹, C. F. Qiao⁵¹, L. Q. Qin¹², X. P. Qin¹³, X. S. Qin⁴, Z. H. Qin^{1,47}, J. F. Qiu¹, S. Q. Qu³⁶, K. H. Rashid⁶¹, K. Ravindran²¹, C. F. Redmer²⁷, A. Rivetti^{62C}, V. Rodin³⁰, M. Rolo^{62C}, G. Rong^{1,51}, Ch. Rosner¹⁵, M. Rump⁵⁶, A. Sarantsev^{28,f}, M. Savrié^{24B}, Y. Schelhaas²⁷, C. Schnier⁴, K. Schoenning⁶³, W. Shan¹⁹, X. Y. Shan^{59,47}, M. Shao^{59,47}, C. P. Shen², P. X. Shen³⁶, X. Y. Shen^{1,51}, H. C. Shi^{59,47}, R. S. Shi^{1,51}, X. Shi^{1,47}, X. D. Shi^{59,47}, J. J. Song⁴⁰, Q. Q. Song^{59,47}, Y. X. Song³⁷, S. Sosio^{62A,62C}, S. Spataro^{62A,62C}, F. F. Sui⁴⁰, G. X. Sun¹, J. F. Sun¹⁶, L. Sun⁶⁴, S. S. Sun^{1,51}, T. Sun^{1,51}, W. Y. Sun³⁴, Y. J. Sun^{59,47}, Y. K. Sun^{59,47}, Y. Z. Sun¹, Z. T. Sun¹, Y. X. Tan^{59,47}, C. J. Tang⁴⁴, G. Y. Tang¹, V. Thoren⁶³, B. Tsednee²⁶, I. Uman^{50D}, B. Wang¹, B. L. Wang⁵¹, C. W. Wang³⁵, D. Y. Wang³⁷, H. P. Wang^{1,51}, K. Wang^{1,47}, L. L. Wang¹, M. Wang⁴⁰, M. Z. Wang³⁷, Meng Wang^{1,51}, W. P. Wang^{59,47}, X. Wang³⁷, X. F. Wang³¹, X. L. Wang^{9,j}, Y. Wang^{59,47}, Y. Wang⁴⁸, Y. D. Wang¹⁵, Y. F. Wang^{1,47,51}, Y. Q. Wang¹, Z. Wang^{1,47}, Z. Y. Wang¹, Ziyi Wang⁵¹, Zongyuan Wang^{1,51}, T. Weber⁴, D. H. Wei¹², P. Weidenkaff²⁷, F. Weidner⁵⁶, H. W. Wen^{34,a}, S. P. Wen¹, D. J. White⁵⁴, U. Wiedner⁴, G. Wilkinson⁵⁷, M. Wolke⁶³, L. Wollenberg⁴, J. F. Wu^{1,51}, L. H. Wu¹, L. J. Wu^{1,51}, X. Wu^{9,j}, Z. Wu^{1,47}, L. Xia^{59,47}, H. Xiao^{9,j}, S. Y. Xiao¹, Y. J. Xiao^{1,51}, Z. J. Xiao³⁴, Y. G. Xie^{1,47}, Y. H. Xie⁶, T. Y. Xing^{1,51}, X. A. Xiong^{1,51}, G. F. Xu¹, J. J. Xu³⁵, Q. J. Xu¹⁴, W. Xu^{1,51}, X. P. Xu⁴⁵, L. Yan^{62A,62C}, W. B. Yan^{59,47}, W. C. Yan⁶⁷, W. C. Yan², H. J. Yang^{41,i}, H. X. Yang¹, L. Yang⁶⁴, R. X. Yang^{59,47}, S. L. Yang^{1,51}, Y. H. Yang³⁵, Y. X. Yang¹², Yifan Yang^{1,51}, Zhi Yang²⁵, M. Ye^{1,47}, M. H. Ye⁷, J. H. Yin¹, Z. Y. You⁴⁸, B. X. Yu^{1,47,51}, C. X. Yu³⁶, G. Yu^{1,51}, J. S. Yu²⁰, T. Yu⁶⁰, C. Z. Yuan^{1,51}, W. Yuan^{62A,62C}, X. Q. Yuan³⁷, Y. Yuan¹, C. X. Yue³², A. Yuncu^{50B,b}, A. A. Zafar⁶¹, Y. Zeng²⁰, B. X. Zhang¹, Guangyi Zhang¹⁶, H. H. Zhang⁴⁸, H. Y. Zhang^{1,47}, J. L. Zhang⁶⁵, J. Q. Zhang⁴, J. W. Zhang^{1,47,51}, J. Y. Zhang¹, J. Z. Zhang^{1,51}, Jianyu Zhang^{1,51}, Jiawei Zhang^{1,51}, L. Zhang¹, Lei Zhang³⁵, S. Zhang⁴⁸, S. F. Zhang³⁵, T. J. Zhang^{41,i},

X. Y. Zhang⁴⁰, Y. Zhang⁵⁷, Y. H. Zhang^{1,47}, Y. T. Zhang^{59,47}, Yan Zhang^{59,47}, Yao Zhang¹, Yi Zhang^{9,j}, Z. H. Zhang⁶, Z. Y. Zhang⁶⁴, G. Zhao¹, J. Zhao³², J. Y. Zhao^{1,51}, J. Z. Zhao^{1,47}, Lei Zhao^{59,47}, Ling Zhao¹, M. G. Zhao³⁶, Q. Zhao¹, S. J. Zhao⁶⁷, Y. B. Zhao^{1,47}, Y. X. Zhao Zhao²⁵, Z. G. Zhao^{59,47}, A. Zhemchugov^{28,c}, B. Zheng⁶⁰, J. P. Zheng^{1,47}, Y. Zheng³⁷, Y. H. Zheng⁵¹, B. Zhong³⁴, C. Zhong⁶⁰, L. P. Zhou^{1,51}, Q. Zhou^{1,51}, X. Zhou⁶⁴, X. K. Zhou⁵¹, X. R. Zhou^{59,47}, A. N. Zhu^{1,51}, J. Zhu³⁶, K. Zhu¹, K. J. Zhu^{1,47,51}, S. H. Zhu⁵⁸, W. J. Zhu³⁶, X. L. Zhu⁴⁹, Y. C. Zhu^{59,47}, Z. A. Zhu^{1,51}, B. S. Zou¹, J. H. Zou¹

(BESIII Collaboration)

¹ *Institute of High Energy Physics, Beijing 100049, People's Republic of China*

² *Beihang University, Beijing 100191, People's Republic of China*

³ *Beijing Institute of Petrochemical Technology, Beijing 102617, People's Republic of China*

⁴ *Bochum Ruhr-University, D-44780 Bochum, Germany*

⁵ *Carnegie Mellon University, Pittsburgh, Pennsylvania 15213, USA*

⁶ *Central China Normal University, Wuhan 430079, People's Republic of China*

⁷ *China Center of Advanced Science and Technology, Beijing 100190, People's Republic of China*

⁸ *COMSATS University Islamabad, Lahore Campus, Defence Road, Off Raiwind Road, 54000 Lahore, Pakistan*

⁹ *Fudan University, Shanghai 200443, People's Republic of China*

¹⁰ *G.I. Budker Institute of Nuclear Physics SB RAS (BINP), Novosibirsk 630090, Russia*

¹¹ *GSI Helmholtzcentre for Heavy Ion Research GmbH, D-64291 Darmstadt, Germany*

¹² *Guangxi Normal University, Guilin 541004, People's Republic of China*

¹³ *Guangxi University, Nanning 530004, People's Republic of China*

¹⁴ *Hangzhou Normal University, Hangzhou 310036, People's Republic of China*

¹⁵ *Helmholtz Institute Mainz, Johann-Joachim-Becher-Weg 45, D-55099 Mainz, Germany*

¹⁶ *Henan Normal University, Xinxiang 453007, People's Republic of China*

¹⁷ *Henan University of Science and Technology, Luoyang 471003, People's Republic of China*

¹⁸ *Huangshan College, Huangshan 245000, People's Republic of China*

¹⁹ *Hunan Normal University, Changsha 410081, People's Republic of China*

²⁰ *Hunan University, Changsha 410082, People's Republic of China*

²¹ *Indian Institute of Technology Madras, Chennai 600036, India*

²² *Indiana University, Bloomington, Indiana 47405, USA*

²³ *(A)INFN Laboratori Nazionali di Frascati, I-00044, Frascati, Italy; (B)INFN and University of Perugia, I-06100, Perugia, Italy*

²⁴ *(A)INFN Sezione di Ferrara, I-44122, Ferrara, Italy; (B)University of Ferrara, I-44122, Ferrara, Italy*

²⁵ *Institute of Modern Physics, Lanzhou 730000, People's Republic of China*

²⁶ *Institute of Physics and Technology, Peace Ave. 54B, Ulaanbaatar 13330, Mongolia*

²⁷ *Johannes Gutenberg University of Mainz, Johann-Joachim-Becher-Weg 45, D-55099 Mainz, Germany*

²⁸ *Joint Institute for Nuclear Research, 141980 Dubna, Moscow region, Russia*

²⁹ *Justus-Liebig-Universitaet Giessen, II. Physikalisches Institut, Heinrich-Buff-Ring 16, D-35392 Giessen, Germany*

³⁰ *KVI-CART, University of Groningen, NL-9747 AA Groningen, The Netherlands*

³¹ *Lanzhou University, Lanzhou 730000, People's Republic of China*

³² *Liaoning Normal University, Dalian 116029, People's Republic of China*

³³ *Liaoning University, Shenyang 110036, People's Republic of China*

³⁴ *Nanjing Normal University, Nanjing 210023, People's Republic of China*

³⁵ *Nanjing University, Nanjing 210093, People's Republic of China*

³⁶ *Nankai University, Tianjin 300071, People's Republic of China*

³⁷ *Peking University, Beijing 100871, People's Republic of China*

³⁸ *Qufu Normal University, Qufu 273165, People's Republic of China*

³⁹ *Shandong Normal University, Jinan 250014, People's Republic of China*

⁴⁰ *Shandong University, Jinan 250100, People's Republic of China*

⁴¹ *Shanghai Jiao Tong University, Shanghai 200240, People's Republic of China*

⁴² *Shanxi Normal University, Linfen 041004, People's Republic of China*

⁴³ *Shanxi University, Taiyuan 030006, People's Republic of China*

⁴⁴ *Sichuan University, Chengdu 610064, People's Republic of China*

⁴⁵ *Soochow University, Suzhou 215006, People's Republic of China*

⁴⁶ *Southeast University, Nanjing 211100, People's Republic of China*

⁴⁷ *State Key Laboratory of Particle Detection and Electronics, Beijing 100049, Hefei 230026, People's Republic of China*

⁴⁸ *Sun Yat-Sen University, Guangzhou 510275, People's Republic of China*

⁴⁹ *Tsinghua University, Beijing 100084, People's Republic of China*

⁵⁰ (A) *Ankara University, 06100 Tandoğan, Ankara, Turkey*; (B) *Istanbul Bilgi University, 34060 Eyüp, İstanbul, Turkey*;

(C) *Uludag University, 16059 Bursa, Turkey*; (D) *Near East University, Nicosia, North Cyprus, Mersin 10, Turkey*

⁵¹ *University of Chinese Academy of Sciences, Beijing 100049, People's Republic of China*

⁵² *University of Hawaii, Honolulu, Hawaii 96822, USA*

⁵³ *University of Jinan, Jinan 250022, People's Republic of China*

⁵⁴ *University of Manchester, Oxford Road, Manchester, M13 9PL, United Kingdom*

⁵⁵ *University of Minnesota, Minneapolis, Minnesota 55455, USA*

⁵⁶ *University of Muenster, Wilhelm-Klemm-Str. 9, 48149 Muenster, Germany*

⁵⁷ *University of Oxford, Keble Rd, Oxford, UK OX13RH*

⁵⁸ *University of Science and Technology Liaoning, Anshan 114051, People's Republic of China*

⁵⁹ *University of Science and Technology of China, Hefei 230026, People's Republic of China*

⁶⁰ *University of South China, Hengyang 421001, People's Republic of China*

⁶¹ *University of the Punjab, Lahore-54590, Pakistan*

⁶² (A) *University of Turin, I-10125, Turin, Italy*; (B) *University of Eastern*

Piedmont, I-15121, Alessandria, Italy; (C) *INFN, I-10125, Turin, Italy*

⁶³ *Uppsala University, Box 516, SE-75120 Uppsala, Sweden*

⁶⁴ *Wuhan University, Wuhan 430072, People's Republic of China*

⁶⁵ *Xinyang Normal University, Xinyang 464000, People's Republic of China*

⁶⁶ *Zhejiang University, Hangzhou 310027, People's Republic of China*

⁶⁷ *Zhengzhou University, Zhengzhou 450001, People's Republic of China*

^a *Also at Ankara University, 06100 Tandoğan, Ankara, Turkey*

^b *Also at Bogazici University, 34342 İstanbul, Turkey*

^c *Also at the Moscow Institute of Physics and Technology, Moscow 141700, Russia*

^d *Also at the Functional Electronics Laboratory, Tomsk State University, Tomsk, 634050, Russia*

^e *Also at the Novosibirsk State University, Novosibirsk, 630090, Russia*

^f *Also at the NRC "Kurchatov Institute", PNPI, 188300, Gatchina, Russia*

^g *Also at Istanbul Arel University, 34295 İstanbul, Turkey*

^h *Also at Goethe University Frankfurt, 60323 Frankfurt am Main, Germany*

ⁱ *Also at Key Laboratory for Particle Physics, Astrophysics and Cosmology, Ministry of Education; Shanghai Key Laboratory for Particle Physics and Cosmology; Institute of Nuclear and Particle Physics, Shanghai 200240, People's Republic of China*

^j *Also at Key Laboratory of Nuclear Physics and Ion-beam Application (MOE) and Institute*

of Modern Physics, Fudan University, Shanghai 200443, People's Republic of China

^k *Also at Harvard University, Department of Physics, Cambridge, MA, 02138, USA*

^l *Currently at: Institute of Physics and Technology, Peace Ave.54B, Ulaanbaatar 13330, Mongolia*

Also at State Key Laboratory of Nuclear Physics and Technology, Peking University, Beijing 100871, People's Republic of China

School of Physics and Electronics, Hunan University, Changsha 410082, China

(Dated: January 7, 2020)

The processes $X(3872) \rightarrow D^{*0}\bar{D}^0 + c.c.$, $\gamma J/\psi$, $\gamma\psi(2S)$, and γD^+D^- are searched for in a 9.0 fb^{-1} data sample collected at center-of-mass energies between 4.178 and 4.278 GeV with the BESIII detector. We observe $X(3872) \rightarrow D^{*0}\bar{D}^0 + c.c.$ and find evidence for $X(3872) \rightarrow \gamma J/\psi$ with statistical significances of 7.4σ and 3.5σ , respectively. No evident signals for $X(3872) \rightarrow \gamma\psi(2S)$ and γD^+D^- are found, and upper limits on the relative branching ratio $R_{\gamma\psi} \equiv \frac{\mathcal{B}(X(3872) \rightarrow \gamma\psi(2S))}{\mathcal{B}(X(3872) \rightarrow \gamma J/\psi)}$ are set at 90% confidence level. Measurements are also reported of the branching ratios for $X(3872) \rightarrow D^{*0}\bar{D}^0 + c.c.$, $\gamma\psi(2S)$, $\gamma J/\psi$, γD^+D^- , as well as the non- $D^{*0}\bar{D}^0$ three-body decays $\pi^0 D^0\bar{D}^0$ and $\gamma D^0\bar{D}^0$, relative to $X(3872) \rightarrow \pi^+\pi^- J/\psi$.

Since the discovery of the $X(3872)$ in 2003 [1] by the Belle Collaboration, many properties of this exotic state have

been reported, including its mass, an upper limit (UL) on its width, and its J^{PC} quantum numbers [2, 3]. The ratio of the branching fraction (BF) of $X(3872) \rightarrow \gamma\psi'$ (This paper uses the notation ψ' to denote the $\psi(2S)$ resonance) to $X(3872) \rightarrow \gamma J/\psi$, $R_{\gamma\psi} \equiv \frac{\mathcal{B}(X(3872) \rightarrow \gamma\psi')}{\mathcal{B}(X(3872) \rightarrow \gamma J/\psi)}$, is predicted to be in the range $(3 \sim 4) \times 10^{-3}$ if the $X(3872)$ is a $D^{*0}\bar{D}^0$ molecule [4, 5], $1.2 \sim 15$ if it is a pure charmonium state [6–12], and $0.5 \sim 5$ if it is a molecule-charmonium mixture [13]. LHCb reported a 4.4σ evidence for the decay $X(3872) \rightarrow \gamma\psi'$ with $R_{\gamma\psi} = 2.46 \pm 0.64 \pm 0.29$ [14], which is in good agreement with the BaBar result $R_{\gamma\psi} = 3.4 \pm 1.4$ [15]. In contrast, the Belle Collaboration reported a negative result with an upper limit of $R_{\gamma\psi} < 2.1$ at the 90% confidence level (C.L.) [16]. The $X(3872)$ is produced at BESIII via the radiative decay from the $Y(4260)$ state [17, 18] with a background level lower than other experiments. This makes BESIII particularly well suited for studies of $X(3872)$ decays to final states containing photons and π^0 mesons.

With BESIII we cannot measure absolute BFs of $X(3872)$ decays since the cross section of $e^+e^- \rightarrow \gamma X(3872)$ is unknown. Instead we determine their ratios to the $\pi^+\pi^-J/\psi$ mode. As discussed in Ref. [4], the BF ratio of $\frac{\mathcal{B}(X(3872) \rightarrow D^{*0}\bar{D}^0 + c.c.)}{\mathcal{B}(X(3872) \rightarrow \pi^+\pi^-J/\psi)}$ can be reliably calculated if the $X(3872)$ is a weakly bound molecule, in which case the ratio is predicted to be around 0.08 for a binding energy of 0.7 MeV. Additionally, the decay width to γD^+D^- is predicted to be 0.2 keV for the molecular case.

In this paper, we report the study of $X(3872) \rightarrow D^{*0}\bar{D}^0$, $\gamma J/\psi$, $\gamma\psi'$, and γD^+D^- using e^+e^- annihilation data collected with the BESIII detector at center-of-mass (CM) energies ranging from 4.178 to 4.278 GeV. The total integrated luminosity is 9.0 fb^{-1} . Charge-conjugate modes are implied throughout. A detailed description of the BESIII detector and the upgrade of the time-of-flight system can be found in Refs. [19, 20].

Simulated samples of events produced with the GEANT4-based [21] Monte Carlo (MC) package, which includes the geometric description of the BESIII detector and the detector response, are used to determine the detection efficiency and to estimate the backgrounds. The simulation includes the beam energy spread and initial-state radiation (ISR) in the e^+e^- annihilations modeled with the generator KKMC [22]. The signal process $e^+e^- \rightarrow \gamma X(3872)$ is generated assuming it is a pure electric dipole (E1) transition, and the subsequent $X(3872)$ decays are generated uniformly in the phase space except $X(3872) \rightarrow \gamma J/\psi$ ($\gamma\psi'$) which is generated assuming a pure E1 transition too. The $X(3872)$ resonance is described with a Flatté formula with parameter values taken from Ref. [23]. An inclusive MC sample, which is 40 times the size of the data sample produced at $\sqrt{s} = 4.178$ GeV, is used to analyze possible backgrounds. The inclusive MC sample consists of open-charm production, ISR production of vector charmonium(-like) states, and continuum processes incorporated in KKMC [22]. The known decay modes

are modeled with EVTGEN [24] using branching fractions taken from the Particle Data Group (PDG) [25], and the remaining unknown decays from charmonium states with LUNDCHARM [26]. Final-state radiation from charged final-state particles are incorporated with the PHOTOS package [27].

Photon and charged-track selections are based on the following criteria. Showers identified as good photon candidates must satisfy fiducial and shower-quality requirements. The minimum EMC energy is 25 MeV for barrel showers, which are within a polar-angle (θ) range of $|\cos \theta| < 0.80$, and 50 MeV for end-cap showers ($0.86 < |\cos \theta| < 0.92$). To eliminate showers produced by charged particles, a photon must be separated by at least 10 degrees from any charged track in the EMC. The time information from the EMC is also used to suppress electronic noise and energy deposits unrelated to the event. For each charged track, the polar angle in the MDC must satisfy $|\cos \theta| < 0.93$, and the point of closest approach to the e^+e^- interaction point must be within ± 10 cm in the beam direction and within ± 1 cm in the plane perpendicular to the beam direction.

When selecting $X(3872) \rightarrow \gamma J/\psi$ decays, we use lepton pairs ($\ell^+\ell^-$, $\ell = e, \mu$) to reconstruct the J/ψ , while for the $X(3872) \rightarrow \gamma\psi'$ selection, we exploit the decays $\psi' \rightarrow \pi^+\pi^-J/\psi$ ($J/\psi \rightarrow \ell^+\ell^-$) and $\psi' \rightarrow \mu^+\mu^-$. The energy deposited in the EMC and the reconstructed momentum in the MDC are used to discriminate the three involved final state particles: pions, muons and electrons. Tracks with momentum less than 1.0 GeV/c are taken as pions while the others are taken as leptons. Lepton candidates with energy deposits in the EMC lower than 0.4 GeV are identified as muons, while those with deposited energy larger than 0.8 GeV are considered to be electrons. The invariant mass of the lepton pair is required to be $\in [m_{J/\psi(\psi')} - 0.02, m_{J/\psi(\psi')} + 0.02] \text{ GeV}/c^2$ for the J/ψ or ψ' selection. We use throughout this paper the notation m_{particle} to represent the mass of the specific particle listed in the PDG [25]. In the case of $X(3872)$ decays to charmed mesons, the $D^{*0} \rightarrow \gamma D^0$ and $\pi^0 D^0$ decays are used to reconstruct the D^{*0} . The D^0 is reconstructed via its $K^-\pi^+$, $K^-\pi^+\pi^0$, and $K^-\pi^+\pi^+\pi^-$ decay modes, while the D^+ is reconstructed via its $K^-\pi^+\pi^+$ and $K^-\pi^+\pi^+\pi^0$ modes. The particle identification (PID) of kaons and pions is based on the dE/dx and TOF information. The probability of the identified particle assumption is required to be larger than the other PID hypotheses.

A vertex fit is performed to ensure that the charged tracks come from a common point. To improve the track momentum and photon energy resolution, and to suppress backgrounds, a kinematic fit is applied to the event with the hypothesis $e^+e^- \rightarrow \gamma X(3872)$ that constrains the sum of four-momentum of the final-state particles to those of the initial colliding beams, with the additional constraints on the masses of the π^0 , D^0 , and D^\pm candidates. When there

are ambiguities due to multi-photon candidates in the same event, we choose the combination with the smallest χ^2 from the kinematic fit. The momenta returned by this kinematic fit are used in the subsequent analysis. The χ^2 of the kinematic fit is required to be less than 40 for $X(3872) \rightarrow \gamma J/\psi$, and less than 60 for the other modes. In addition, the χ^2 of the kinematic fit of the hypothesis under study should be smaller than those for hypotheses with extra or fewer photons. For channels with two radiative photons, we denote the photon with larger energy after the kinematic fit as γ_H and the other γ_L . In these decays, π^0 and η vetoes are imposed on the invariant mass of the photon pair, $M(\gamma_L \gamma_H)$ to suppress further the possible π^0 and η background, *i.e.*, $M(\gamma_L \gamma_H) \notin [m_{\pi^0} - 0.020, m_{\pi^0} + 0.020] \text{ GeV}/c^2$ and $\notin [m_\eta - 0.030, m_\eta + 0.030] \text{ GeV}/c^2$.

For the decay $X(3872) \rightarrow \gamma J/\psi$, studies performed on the inclusive MC sample indicate that the dominant backgrounds are Bhabha and di-muon events for $J/\psi \rightarrow e^+ e^-$ and $\mu^+ \mu^-$, respectively. To suppress Bhabha events in the $J/\psi \rightarrow e^+ e^-$ selection, the cosine of the polar angle of the selected photons, $\cos \theta$, is required to be within $[-0.7, 0.7]$. Background from $e^+ e^- \rightarrow \gamma \chi_{c1,2}$ with $\chi_{c1,2} \rightarrow \gamma J/\psi$ is suppressed by requiring $|M(\gamma_L J/\psi) - m_{\chi_{c1,2}}| > 0.02 \text{ GeV}/c^2$. No peaking structure is found in the $M(\gamma_{H/L} J/\psi)$ spectra. Here, $M(\gamma_{H/L} J/\psi) \equiv M(\gamma_{H/L} \ell^+ \ell^-) - M(\ell^+ \ell^-) + m_{J/\psi}$.

To determine the number of signal events, a simultaneous fit is performed on the mass spectra of $\gamma_H J/\psi$ with $J/\psi \rightarrow \mu^+ \mu^-$ and $e^+ e^-$. Throughout this paper, we use an unbinned maximum-likelihood fit as the nominal fit method. Assuming that the $X(3872)$ signal is entirely produced via $Y(4260)$ decays whose parameters are taken from Ref. [25], we compute the averaged reconstruction efficiency for the sum of the data samples. The ratio of signal yields for $\mu^+ \mu^-$ and $e^+ e^-$ modes is constrained to the product of the corresponding BFs and weighted reconstruction efficiencies. In the fit, the signal distributions are described with shapes obtained from the MC simulation, and the backgrounds are described with a second-order Chebyshev polynomial. The distributions of $M(\gamma_H J/\psi)$ as well as the fit results are shown in Fig. 1(a). The statistical significance for $X(3872) \rightarrow \gamma J/\psi$ is always greater than 3.5σ , evaluated with a range of alternative background shapes. The significance is calculated by comparing the likelihoods with and without the signal components included, and taking the change in the number of degrees of freedom (ndf) into account. The fit yields 38.8 ± 11.9 and 18.4 ± 5.6 $X(3872) \rightarrow \gamma J/\psi$ events, for $J/\psi \rightarrow \mu^+ \mu^-$ and $e^+ e^-$, respectively, corresponding to $(20.1 \pm 6.2) \times 10^2$ BF- and efficiency-corrected $X(3872) \rightarrow \gamma J/\psi$ events. The goodness of the fit is $\chi^2/\text{ndf} = 46.9/68$ ($p = 0.98$).

For the decay $X(3872) \rightarrow \gamma \psi'$ with $\psi' \rightarrow \mu^+ \mu^-$, the selection criteria for $\psi' \rightarrow \mu^+ \mu^-$ are the same as those for $J/\psi \rightarrow \mu^+ \mu^-$. For the $\psi' \rightarrow \pi^+ \pi^- J/\psi$ channel, we take events satisfying $M(\pi^+ \pi^- J/\psi) \equiv M(\pi^+ \pi^- \ell^+ \ell^-) - M(\ell^+ \ell^-) + m_{J/\psi} \in [m_{\psi'}, -0.006, m_{\psi'} + 0.006] \text{ GeV}/c^2$ as

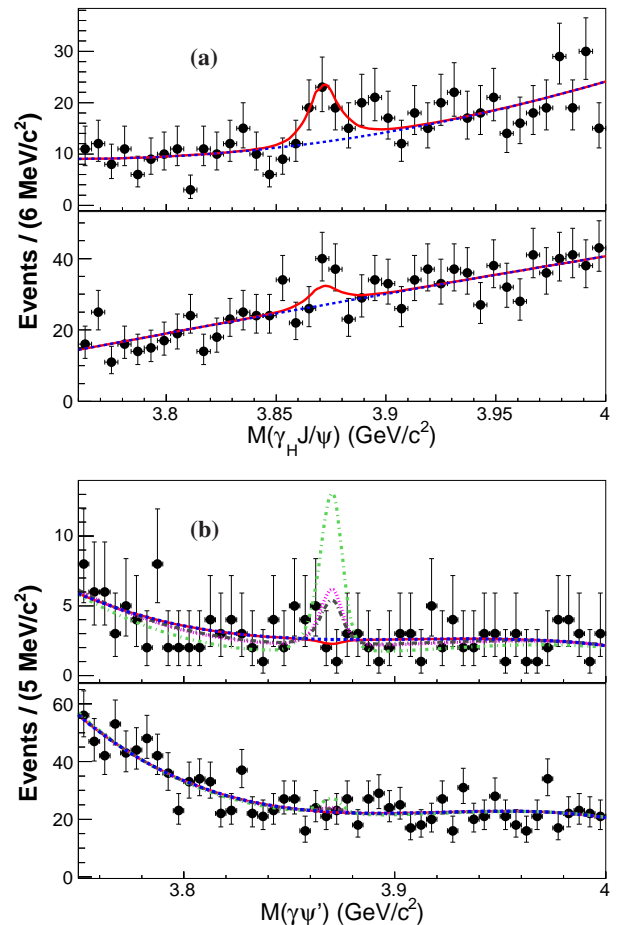


FIG. 1. (a) Fit results for $X(3872) \rightarrow \gamma J/\psi$ where the top panel is for the $\mu^+ \mu^-$ mode and the bottom for the $e^+ e^-$ mode. (b) Fit results for $X(3872) \rightarrow \gamma \psi'$ where the top panel is for the $\pi^+ \pi^- J/\psi$ mode and the bottom for the $\mu^+ \mu^-$ mode. The points with error bars are from data, the red curves are the best fit (color online). In (b), the rose-red dotted line are the fits with the signal constrained to the expectation using $X(3872) \rightarrow \pi^+ \pi^- J/\psi$ based on the relative ratios taken from a global fit [29]; the green dash-dotted lines are using $X(3872) \rightarrow \gamma J/\psi$ as the reference based on the LHCb measurement [14], and the grey long dashed lines are using $X(3872) \rightarrow \gamma J/\psi$ as the reference based on the Belle measurement [16].

the signal-event candidates. The main background is $e^+ e^- \rightarrow \pi^+ \pi^- \psi'$, with $\psi' \rightarrow \gamma \gamma J/\psi$. We require $M(\pi^+ \pi^-)_{\text{recoil}} \notin [m_{\psi'} - 0.01, m_{\psi'} + 0.01] \text{ GeV}/c^2$ to suppress these events, where $M(\pi^+ \pi^-)_{\text{recoil}}$ is the recoiling mass of the $\pi^+ \pi^-$ system.

To determine the number of $X(3872) \rightarrow \gamma \psi'$ decays, similar fits are performed to the corrected mass $M(\gamma \pi^+ \pi^- J/\psi)$ and $M(\gamma \psi')$ as described above. The distribution of $M(\gamma \psi')$ as well as the fitting results are shown in Fig. 1(b). The fit yields -0.9 ± 4.1 and -0.4 ± 1.6 $X(3872) \rightarrow \gamma \psi'$ events with $\psi' \rightarrow \pi^+ \pi^- J/\psi$ and $\mu^+ \mu^-$, respectively, corresponding to $(-1.1 \pm 5.2) \times 10^2$ BF- and efficiency-corrected $X(3872)$ events, and the goodness of the

fit is $\chi^2/\text{ndf} = 45.0/58$ ($p = 0.89$). The UL of the number of produced events (N_{UL}) is estimated to be 10.0×10^2 at the 90% C.L., by finding the solution of

$$\int_0^{N_{\text{UL}}} \mathcal{L}(N) dN / \int_0^{\infty} \mathcal{L}(N) dN = 90\%,$$

where $\mathcal{L}(N)$ is the likelihood distribution in various number of BF- and efficiency-corrected $X(3872)$ events (N). By sampling the likelihood distributions of $N_{\text{prod}}(\gamma\psi')$ and $N_{\text{prod}}(\gamma J/\psi)$, the UL of the $R_{\gamma\psi}$ is determined to be 0.59 at the 90% C.L. where the common systematic uncertainties cancel out.

We also perform fits where the signal contribution is fixed to the expectation calculated from previous measurements. We fix the cross-section of $e^+e^- \rightarrow \gamma X(3872)$, $X(3872) \rightarrow \pi^+\pi^- J/\psi$ production to the value reported in Ref. [17] and take the relative ratio $\frac{\mathcal{B}(X(3872) \rightarrow \gamma\psi')}{\mathcal{B}(X(3872) \rightarrow \pi^+\pi^- J/\psi)}$ from a global fit [29], or fix $X(3872) \rightarrow \gamma J/\psi$ to our own result and take $R_{\gamma\psi}$ from an LHCb measurement [14], and from a Belle measurement [16]. The results, also shown in Fig. 1(b), have a goodness-of-fit of $\chi^2/\text{ndf} = 46.9/59$ ($p = 0.87$), $66.8/59$ ($p = 0.23$), and $46.0/59$ ($p = 0.89$) for the BESIII, LHCb and Belle hypotheses, respectively. Our result for $R_{\gamma\psi}$ is 2.8σ lower than that reported by the LHCb collaboration, corresponding to a p -value of 0.0048 calculated with $p = \int_0^{\infty} \int_{R_0}^{\infty} \mathcal{L}(R) G(R_0) dR dR_0$, where $\mathcal{L}(R)$ is the likelihood distribution in this work and $G(R)$ is the Gaussian-assumed likelihood profile of the uncertainty of LHCb measurement.

We consider the possibility of non-resonant three-body production to the final states $\gamma D^0 \bar{D}^0$ and $\pi^0 D^0 \bar{D}^0$, in addition to the well-established decay $X(3872) \rightarrow D^{*0} \bar{D}^0$. The mass spectra $M(\gamma D^0 \bar{D}^0)$ and $M(\pi^0 D^0 \bar{D}^0)$ are shown in Fig. 2 for the case when $M(\gamma\pi^0 D)$ lies in (a) or out of (b) the D^{*0} mass region, and when $M(\pi^0 D^0 \bar{D}^0)$ lies in this mass range (c). We fit the two mass spectra individually, and determine the signal yields to be $N_{\gamma D^0 \bar{D}^0}^{\text{in}} = 17.5 \pm 6.3$, $N_{\gamma D^0 \bar{D}^0}^{\text{out}} = 4.3 \pm 2.2$, and $N_{\pi^0 D^0 \bar{D}^0}^{\text{in}} = 35.4 \pm 7.6$, where the superscript indicates the mass range under consideration, and the subscript the final state. Note that there are overlaps between the three- and two-body decays on the $M(\gamma(\pi^0) D^0 \bar{D}^0)$ distribution, thus the results from the fits are not the true yields in each category. We use these fit results, and an efficiency matrix determined from MC simulation that accounts for migrations of true events between the mass ranges, to determine the number of produced events in each category. The efficiency-corrected yields for non-resonant three-body $X(3872) \rightarrow \gamma D^0 \bar{D}^0$ production and the decay $X(3872) \rightarrow D^{*0} \bar{D}^0$ ($D^{*0} \rightarrow \gamma D^0$) events are found to be 1.3 ± 0.7 and 20.5 ± 7.4 , respectively, and the corresponding yields for $X(3872) \rightarrow \pi^0 D^0 \bar{D}^0$ and $X(3872) \rightarrow D^{*0} \bar{D}^0$ ($D^* \rightarrow \pi^0 D^0$) decays are -0.5 ± 2.3 and 36.1 ± 7.7 , respectively. The yields for the three-body decays are not significant and so we set ULs at the 90% C.L. of 8.7 events for $X(3872) \rightarrow \gamma D^0 \bar{D}^0$ and 2.3 events

for $X(3872) \rightarrow \pi^0 D^0 \bar{D}^0$, corresponding to 3.2×10^2 and 1.2×10^2 BF- and efficiency- corrected events, respectively. Here systematic uncertainties, which are discussed later, are taken into account.

In the next stage of the analysis of the $X(3872) \rightarrow D^{*0} \bar{D}^0$ decays, the combination of γD^0 or $\pi^0 D^0$ with an invariant mass closest to the D^{*0} nominal mass is taken as the D^{*0} candidate. For the channel $D^{*0} \rightarrow \gamma D^0$, the mass window for selecting the D^{*0} is $M(\gamma_L D) \in [m_{D^{*0}} - 0.006, m_{D^{*0}} + 0.006] \text{ GeV}/c^2$, while for $D^{*0} \rightarrow \pi^0 D^0$ it is $M(\pi^0 D^0) \in [m_{D^{*0}} - 0.004, m_{D^{*0}} + 0.004] \text{ GeV}/c^2$. The distributions of the corrected invariant mass $M(D^{*0} \bar{D}^0) \equiv M(\gamma(\pi^0) D^0 \bar{D}^0) - M(\gamma(\pi^0) D) + m_{D^{*0}}$ are shown in Fig. 2(d,e) following these requirements, where contributions from non-resonant three-body processes are neglected.

To measure the $X(3872) \rightarrow D^{*0} \bar{D}^0$ signal, a simultaneous fit is performed to the corrected invariant-mass distributions. The ratio of the signal yields for $D^{*0} \rightarrow \gamma D^0$ and $\pi^0 D^0$ is constrained to the product of corresponding BFs and averaged reconstruction efficiencies. The signals are represented by MC simulated shapes, and the backgrounds by ARGUS functions [28], with thresholds fixed at $m_{D^{*0}} + m_{\bar{D}^0}$. The fit results are shown in Fig. 2(d,e). The number of signal events are 20.2 ± 3.6 and 25.5 ± 4.6 from the $D^{*0} \rightarrow \gamma D$ and $\pi^0 D$ modes, respectively, corresponding to $(30.0 \pm 5.4) \times 10^3$ efficiency- and BF-corrected $X(3872) \rightarrow D^{*0} \bar{D}^0$ events. The goodness-of-fit is $\chi^2/\text{ndf} = 13.0/16$ ($p = 0.67$) after rebinning the data to satify the criterion that there are at least seven events in one bin. Varying the fit range and describing the background with alternative shapes always results in a signal fit that has a statistical significance greater than 7.4σ .

The invariant mass of the $\gamma D^+ D^-$ system following the $X(3872) \rightarrow \gamma D^+ D^-$ selection is shown in Fig. 2(f). No evident $X(3872)$ signal is found. This conclusion is quantified by performing an unbinned maximum-likelihood fit to the invariant-mass distribution, in which the signal component is described by a MC-simulated shape and the background is represented by a second-order polynomial. The goodness-of-fit is $\chi^2/\text{ndf} = 6.2/5$ ($p = 0.29$). The fit yields $(0.0^{+0.5}_{-0.0}) X(3872)$ events. The UL on the number of the produced $X(3872) \rightarrow \gamma D^+ D^-$ is 2.8×10^3 events at the 90% C.L., with systematic uncertainties included in the calculation.

The sources of the systematic uncertainties considered in the analysis are listed in Table I. The uncertainties associated with the knowledge of the tracking efficiency (1% per track), photon detection (1% per photon), PID (1% per track), luminosity (1%), π^0 reconstruction (1% per π^0) are assigned following the results of earlier BESIII studies [30–32]. The uncertainties listed for the modes involving D^0 and D^+ mesons are calculated considering the correlations between the different decay channels used to reconstruct these states. The uncertainties on the BFs of the D meson, J/ψ , and ψ'

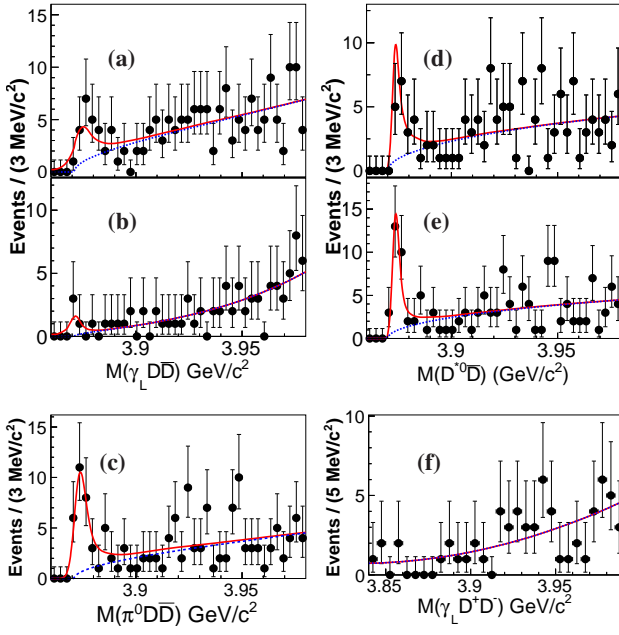


FIG. 2. Left column: $M(\gamma D^0 \bar{D}^0)$ with $M(\gamma D)$ in (a) or below the D^{*0} mass window. $M(\pi^0 D^0 \bar{D}^0)$ with $M(\pi^0 D)$ in the D^{*0} mass window (c). Right column: Simultaneous fit results for $X(3872) \rightarrow D^{*0} \bar{D}^0$ with $D^{*0} \rightarrow \gamma D^0$ (d) and $D^{*0} \rightarrow \pi^0 D^0$ mode (e). Fit results for $X(3872) \rightarrow \gamma D^+ D^-$ (f). The points with error bars are from data, the red curves are the best fit, and the blue dashed curves are the background components (color online).

decays are taken from Ref. [25].

The uncertainty associated with the mass window used to select J/ψ mesons, which arises from a difference in resolution between data and MC, is 1.6% [17], and that for selecting D mesons is 0.7% per D meson [33]. There are various mass windows in our analysis to veto backgrounds. These background processes, *e.g.*, $e^+e^- \rightarrow \eta J/\psi$, $e^+e^- \rightarrow \pi^+\pi^- \psi' (\psi' \rightarrow \pi^+\pi^- J/\psi)$, $e^+e^- \rightarrow \gamma \chi_{c1,2} (\chi_{c1,2} \rightarrow \gamma J/\psi)$, have been studied in other analyses, and the MC simulation found to exhibit a similar mass resolution to the data. For this reason, and because these backgrounds enter our sample at a very low level, no systematic uncertainty is assigned for residual discrepancies. The systematic uncertainty associated with the efficiency of the kinematic fit is estimated using the method discussed in Ref. [34].

To assign the systematic uncertainty associated with the MC events generation, we take the change in reconstruction efficiency when varying the assumption of an E1 transition in $e^+e^- \rightarrow \gamma X(3872)$ and $X(3872) \rightarrow \gamma J/\psi (\psi')$ decays to pure phase space. We change the energy-dependent cross-section lineshape of the $Y(4260)$ [25] in the generator to the measured $e^+e^- \rightarrow \gamma X(3872)$ [18] lineshape and the difference on the Born cross section is taken as the systematic uncertainty due to the ISR correction. To estimate the uncertainty arising from the limited knowledge of the

background shapes, we vary the shapes to different order of polynomials in the fit, and change the fit range at the same time. To incorporate the systematic uncertainty in to the UL, the most conservative result in the various fits is taken as the final result. The effects on the modeling of the signal shapes from discrepancies between the mass resolution in data and MC simulation are negligible.

A summary of the systematic uncertainties is presented in Table I, and the total systematic uncertainty is obtained by adding the individual components in quadrature.

TABLE I. Summary of the systematic uncertainties in the cross-section measurements (in %). Symbols “-” the cases where the uncertainties are already incorporated in UL estimations.

| Sources | $\gamma J/\psi$ | $\gamma \psi'$ | $\gamma D^0 \bar{D}^0$ | $\pi^0 D^0 \bar{D}^0$ | $D^{*0} \bar{D}^0$ | $\gamma D^+ D^-$ |
|----------------|-----------------|----------------|------------------------|-----------------------|--------------------|------------------|
| Luminosity | 1.0 | 1.0 | 1.0 | 1.0 | 1.0 | 1.0 |
| Tracking | 2 | 4 | 5.3 | 5.3 | 5.3 | 6 |
| Photon | 2 | 2 | 1.4 | 3.1 | 4.4 | 2.5 |
| PID | 0 | 0 | 5.3 | 5.3 | 5.3 | 6 |
| π^0 | 0 | 0 | 0.3 | 1.2 | 1.5 | 2.7 |
| BFs | 0.5 | 1.9 | 3.9 | 3.9 | 6.4 | 3.7 |
| mass window | 1.6 | 1.6 | 1.4 | 1.4 | 1.4 | 1.4 |
| Kinematic fit | 1.0 | 1.0 | 3.3 | 3.3 | 3.3 | 3.9 |
| ISR correction | 6.5 | 2.9 | 17.5 | 13.7 | 13.2 | 10.8 |
| Generator | 3.3 | 3.2 | 2.2 | 2.2 | 2.2 | 2.2 |
| Background | 11.5 | - | 14.3 | 17.5 | 14.5 | - |
| Total | 14.1 | 6.8 | 24.6 | 22.2 | 22.8 | 15.5 |

The decay channel $X(3872) \rightarrow \pi^+\pi^- J/\psi$ is reconstructed [17, 18] to provide a normalization mode against which the rates of the other decays can be compared. This channel yields 93.9 ± 11.4 $X(3872) \rightarrow \pi^+\pi^- J/\psi$ events, corresponding to $(24.9 \pm 3.0) \times 10^2$ BF- and efficiency-corrected events. The relative ratios can then be obtained by sampling the number of produced events of $\gamma J/\psi$, $\gamma \psi'$, $\gamma D^0 \bar{D}^0$, $\pi^0 D^0 \bar{D}^0$, $D^{*0} \bar{D}^0$, and $\gamma D^+ D^-$ according to the likelihood distributions, compared with that of $\pi^+\pi^- J/\psi$. We convolute the distributions with a Gaussian whose width is the systematic uncertainty of each channel, where uncertainties in common with the $\pi^+\pi^- J/\psi$ channel are excluded. The ratios are listed in Table II for the modes studied in this paper, together with $X(3872) \rightarrow \omega J/\psi$ and $\pi^0 \chi_{c1}$, whose production rates have recently been measured by BESIII [18, 35].

In summary, using e^+e^- collision data taken at $\sqrt{s} = 4.178\text{--}4.278$ GeV, we observe $X(3872) \rightarrow D^{*0} \bar{D}^0 + c.c.$ and find evidence for $X(3872) \rightarrow \gamma J/\psi$ with significances of 7.4σ and 3.5σ , respectively. No evidence is found for the decays $X(3872) \rightarrow \gamma \psi'$ and $X(3872) \rightarrow \gamma D^+ D^-$. The UL on the ratio $R_{\gamma\psi} < 0.59$ is obtained at the 90% C.L., which is inconsistent with LHCb measurement [14] but consistent with the Belle measurement [16] and the global fit [29]. Our measurement indicates that the $X(3872)$ state is not likely a conventional charmonium state but rather a molecule or a mixture of molecule and charmonium. We also measure the ratios of BFs for $X(3872) \rightarrow \gamma J/\psi$, $\gamma \psi'$,

TABLE II. Relative branching ratios and UL on branching ratios compared with $X(3872) \rightarrow \pi^+ \pi^- J/\psi$.

| mode | $\gamma J/\psi$ | $\gamma \psi'$ | $\gamma D^0 \bar{D}^0$ | $\pi^0 D^0 \bar{D}^0$ | $D^{*0} \bar{D}^0 + c.c.$ | $\gamma D^+ D^-$ | $\omega J/\psi$ | $\pi^0 \chi_{c1}$ |
|-------|-----------------|------------------|------------------------|-----------------------|---------------------------|------------------------|----------------------------------|--------------------------------------|
| ratio | 0.79 ± 0.28 | -0.03 ± 0.22 | 0.54 ± 0.48 | -0.13 ± 0.47 | 11.77 ± 3.09 | $0.00^{+0.48}_{-0.00}$ | $1.6^{+0.4}_{-0.3} \pm 0.2$ [18] | $0.88^{+0.33}_{-0.27} \pm 0.10$ [35] |
| UL | - | < 0.42 | < 1.58 | < 1.16 | - | < 0.99 | - | - |

$\gamma D^0 \bar{D}^0$, $\pi^0 D^0 \bar{D}^0$, $D^{*0} \bar{D}^0 + c.c.$, and $\gamma D^+ D^-$ to that for $X(3872) \rightarrow \pi^+ \pi^- J/\psi$. As discussed in Ref. [4], the relative ratios can be calculated on the assumption that the $X(3872)$ is a bound state of $D^{*0} \bar{D}^0$. We note, however, that no predictions are yet available for a binding energy of (0.01 ± 0.20) MeV, which is the value that is obtained from the most recent mass measurements [25]. Our measurement provides essential input to future tests of the molecular model for the $X(3872)$ meson.

The BESIII collaboration thanks the staff of BEPCII and the IHEP computing center for their strong support. This work is supported in part by National Key Basic Research Program of China under Contract No. 2015CB856700; National Natural Science Foundation of China (NSFC) under Contracts Nos. 11905179, 11625523, 11635010, 11735014, 11822506, 11835012, 11961141012; the Chinese Academy of Sciences (CAS) Large-Scale Scientific Facility Program; Joint Large-Scale Scientific Facility Funds of the NSFC and CAS under Contracts Nos. U1532257, U1532258, U1732263, U1832207; CAS Key Research Program of Frontier Sciences under Contracts Nos. QYZDJ-SSW-SLH003, QYZDJ-SSW-SLH040; 100 Talents Program of CAS; INPAC and Shanghai Key Laboratory for Particle Physics and Cosmology; ERC under Contract No. 758462; German Research Foundation DFG under Contracts Nos. Collaborative Research Center CRC 1044, FOR 2359; Istituto Nazionale di Fisica Nucleare, Italy; Ministry of Development of Turkey under Contract No. DPT2006K-120470; National Science and Technology fund; STFC (United Kingdom); The Knut and Alice Wallenberg Foundation (Sweden) under Contract No. 2016.0157; The Royal Society, UK under Contracts Nos. DH140054, DH160214; The Swedish Research Council; U. S. Department of Energy under Contracts Nos. DE-FG02-05ER41374, DE-SC-0010118, DE-SC-0012069

- [6] T. Barnes, S. Godfrey, and E.S. Swanson, Phys. Rev. D **72**, 054026 (2005).
- [7] T. Barnes and S. Godfrey, Phys. Rev. D **69**, 054008 (2004).
- [8] B.Q. Li and K.T. Chao, Phys. Rev. D **79**, 094004 (2009).
- [9] T. Lahde, Nucl. Phys. A **714**, 183 (2003).
- [10] A.M. Badalov, V.D. Orlovsky, Y.A. Simonov, and B.L.G. Bakker, Phys. Rev. D **85**, 114002 (2012).
- [11] T. Mehen and R. Springer, Phys. Rev. D **83**, 094009 (2011).
- [12] T.M. Wang and G.L. Wang, Phys. Lett. B **697**, 3 (2011).
- [13] E. J. Eichten, K. Lane, and C. Quigg, Phys. Rev. D **73**, 014014 (2006).
- [14] R. Aaij *et al.* [LHCb Collaboration], Nucl. Phys. B **886**, 665 (2014).
- [15] B. Aubert *et al.* [BaBar Collaboration], Phys. Rev. Lett. **102**, 132001 (2009).
- [16] V. Bhardwaj *et al.* [Belle Collaboration], Phys. Rev. Lett. **107**, 091803 (2011).
- [17] M. Ablikim *et al.* [BESIII Collaboration], Phys. Rev. Lett. **112**, 092001 (2014).
- [18] M. Ablikim *et al.* [BESIII Collaboration], Phys. Rev. Lett. **122**, 232002 (2019).
- [19] M. Ablikim *et al.* [BESIII Collaboration], Nucl. Instrum. Meth. A **614**, 345 (2010).
- [20] X. Li *et al.*, Radiat. Detect. Technol. Methods **1**, 13 (2017); Y.X. Guo *et al.*, Radiat. Detect. Technol. Methods **1**, 15 (2017).
- [21] S. Agostinelli *et al.* [GEANT4 Collaboration], Nucl. Instrum. Meth. A **506**, 250 (2003).
- [22] S. Jadach, B.F.L. Ward, and Z. Was, Comput. Phys. Commun. **130**, 260 (2000); Phys. Rev. D **63**, 113009 (2001).
- [23] O. Zhang, C. Meng and H.Q. Zheng, Phys. Lett. B **680**, 453 (2009).
- [24] D.J. Lange, Nucl. Instrum. Meth. A **462**, 152 (2001); R.G. Ping, Chin. Phys. C **32**, 599 (2008).
- [25] M. Tanabashi *et al.* [Particle Data Group], Phys. Rev. D **98**, 030001 (2018).
- [26] J.C. Chen, G.S. Huang, X.R. Qi, D.H. Zhang and Y.S. Zhu, Phys. Rev. D **62**, 034003 (2000); R.L. Yang, R.G. Ping and H. Chen, Chin. Phys. Lett. **31**, 061301 (2014).
- [27] P. Golonka, and Z. Was, Eur. Phys. J. C **45**, 97 (2006).
- [28] H. Albrecht *et al.* [ARGUS Collaboration], Phys. Lett. B **241**, 278 (1990).
- [29] C. Li and C. Z. Yuan, Phys. Rev. D **100**, no. 9, 094003 (2019).
- [30] M. Ablikim *et al.* [BESIII Collaboration], Chin. Phys. C **39**, 093001 (2015).
- [31] M. Ablikim *et al.* [BESIII Collaboration], Phys. Rev. D **93**, 011102 (2016).
- [32] M. Ablikim *et al.* [BESIII Collaboration], Phys. Rev. D **87**, 012002 (2013).
- [33] M. Ablikim *et al.* [BESIII Collaboration], Phys. Rev. Lett. **122**, 102002 (2019).
- [34] M. Ablikim *et al.* [BESIII Collaboration], Phys. Rev. D **87**, 012002 (2013).
- [35] M. Ablikim *et al.* [BESIII Collaboration], Phys. Rev. Lett. **122**, 202001 (2019).